Bachelor Project

Czech
Technical
University
in Prague

F3

Faculty of Electrical Engineering
Department of Microelectronics

Atomic Layer Deposition

Karolína Veselá

Supervisor: doc. RNDr. Jan Voves, CSc.
Field of study: Open Electronic Systems
May 2021

Acknowledgements

I would like to thank Jan Voves for the opportunity of being part of the ALD research group, for his kind guidance and expert management of this thesis. I am also grateful to Alexandr Pošta for his help and patience in showing me around the laboratory. Furthermore, I must thank my amazing classmates Erik Rapp and Martin Šimák for their friendship and support throughout my studies.

Declaration

I declare that I completed the presented thesis independently and that all used sources are quoted in accordance with the Methodological instructions that cover the ethical principles for writing an academic thesis.

In Prague, 18. May 2021

Prohlašuji, že jsem předloženou práci vypracovala samostatně, a že jsem uvedla veškeré použité informační zdroje v souladu s Metodickým pokynem o dodržování etických principů při přípravě vysokoškolských závěrečných prací.

V Praze, 18. květen 2021

Abstract

Development in the microelectronic industry leads to the scaling down of semiconductor devices; hence, a need for thin, perfect layers of materials arose. The application of atomic layer deposition (ALD) has sparked a good deal of interest due to its benefits compared to other traditional thin film deposition techniques. ALD is a chemical gas phase deposition method based on sequential, self-saturating surface reactions, which gradually forms monolayers of new material. The thesis introduces ALD with its basic principles and applications. It focuses on a commercial ALD system manufactured by SENTECH Instruments GmbH and its mechanics. In the experimental part, the growth of Al_2O_3 and SiO_2 thin films is performed on Si wafers and on an aluminum electrode. The deposited samples are examined by Raman spectroscopy and AFM.

Keywords: atomic layer deposition, vapor phase epitaxy, nanotechnology, thin film growth

Supervisor: doc. RNDr. Jan Voves, CSc.
Faculty of Electrical Engineering,
Czech Technical University in Prague,
Technická 2,
Praha 6

Abstrakt

Rozvoj mikroeletrotechnického průmyslu vede ke zmenšování rozměrů polovodičových součástek, a proto vyvstává poptávka po materiálech z tenkých vrstev. Využití metody depozice atomárních vrstev přineslo vlnu zájmu díky jejím výhodám oproti tradičním depozičním technikám. ALD je chemická metoda depozice z plynné fáze založená na opakovaných samo-nasycovacých povrchových reakcích, které postupně formují jednotlivé vrstvy nového materiálu. Tato bakalářská práce představuje ALD, její základní principy a aplikace. Dále se zaměřuje na komerční ALD stroj vyráběný firmou SENTECH Instruments GmbH a jeho mechaniku. V experimentální části je proveden růst tenkých vrstev Al_2O_3 a SiO_2 na křemíkovou polovodičovou desku a na hliníkovou elektrodu. Vytvořené vzorky jsou zkoumány Ramanovou spektroskopií a AFM.

Klíčová slova: depozice atomárních vrstev, epitaxe z plynné fáze, nanotechnologie, růst tenkých vrstev

Překlad názvu: Depozice atomárních vrstev

Contents

1 Introduction **1**

2 Basics of Atomic Layer Deposition **3**

2.1 A Typical ALD Cycle 3

2.2 Characteristics and Advantages of ALD 5

2.3 Precursors and Co-reactants 7

2.4 Modified ALD Techniques 9

3 ALD Applications **11**

3.1 FinFETs and high mobility FETs 12

3.2 Non-volatile Memory (NVM) Devices 13

4 SENTECH SI PEALD LL System **15**

4.1 Brief View on ALD Market 15

4.2 SENTECH's ALD Performance . 17

4.3 SI PEALD LL Description 18

4.3.1 Reactor Unit 20

4.3.2 Precursor and Gas Cabinet . . 21

4.3.3 Hardware and Software Control 22

4.3.4 Real Time Monitor 23

5 Experimental Part **25**

5.1 Preparation 25

5.2 Trial PEALD Growth of Thin Oxide Layers 27

5.3 Characterization Methods 28

5.3.1 Raman Spectroscopy 28

5.3.2 Atomic Force Microscopy . . . 29

5.4 Results and Discussion 30

5.5 Capacitor Experiment 32

6 Conclusions **37**

Bibliography **39**

Project Specification **43**

Figures

2.1 Schematics of one ALD cycle. [3] 4

2.2 ALD coating of trenches. [2] 5

3.1 Schematic drawing of FinFET. [4] 12

3.2 Different gate design structures with the use of ALD. (a) FinFET transistor, (b) Omega-gate structure wrapping around a Ge channel, (c) Pi-gate surrounding a Si nanowire. [1] 12

3.3 (a) Schematic drawing of NC memory and (b) TEM image of HfAlO/W/HfAlO structure of NCs embedded in HfAlO. [4] 14

4.1 Properties of thermal ALD (a) layer thickness, (b) refractive index uniformity. [10] 17

4.2 Properties of PEALD (a) layer thickness, (b) refractive index uniformity. [10] 17

4.3 Linearity of growth. [10] 18

4.4 SI PEALD LL system. [10] 19

4.5 SI PEALD LL Reactor unit with RTM. [11] 20

4.6 Direct draw (left) and bubble draw (right) precursor containers and their installation. [13] 21

4.7 Reactor chamber and plasma source schematics. [11] 22

4.8 ALD system software example. [10] 23

4.9 PEALD with ellipsometer and the principle of ellipsometry analysis. [10] 24

4.10 Real time monitoring of TiO_2 deposition. [11] 24

5.1 Front view of the glovebox connected to PEALD. [2] 26

5.2 Side view of PEALD. [2] 26

5.3 (a) Renishaw's Raman spectrometer [22], (b) NTEGRA atomic force microscopy device. [25] 28

5.4 Laser beam deflection for AFM. [2] 29

5.5 (a) original Si wafer, (b) wafer with Al_2O_3 thin film (c) wafer with SiO_2 thin film. 30

5.6 Raman spectrum of Al_2O_3 film measured with 633 nm laser. 31

5.7 Raman spectrum of plain Si wafer measured with 532 nm laser. 31

5.8 AFM diagram of (a) real surface scan of Al_2O_3 and (b) flattened diagram of the surface in 3D form. 32

5.9 AFM diagram of (a) real surface scan of SiO_2 and (b) flattened diagram of the surface in 3D form. 32

5.10 The border between Al and Al_2O_3 with tape impurities under regular microskope: (a) for 20 nm sample (b) for 100 nm sample. 33

5.11 AFM diagram of (a) the Al_2O_3 layer and (b) the border between Al and Al_2O_3 with tape impurities. . . 34

5.12 Height profile of the surface of the 20 nm capacitor. 34

5.13 Height profile of the surface of the 100 nm sample with Al_2O_3 coating. 34

5.14 The four samples after the second Al layer deposition. 35

5.15 (a) Photo of the sample with 20 nm functional capacitor. (b) The 20 nm capacitor under Raman microscope. 35

Tables

2.1 Overview of the materials prepared by ALD. [5] 7

5.1 PEALD dosing and waiting times 27

5.2 Samples' PEALD characteristics 33

Introduction

Atomic layer deposition (ALD) is a vapor phase technique capable of depositing a variety of nano-thin film materials. At first, ALD was not expected to play a significant role in the electronic industry, mainly due to its low growth rate. However, since the requirements for smaller and more sophisticated structures have not ceased, ALD-grown thin films have slowly attracted the attention of many technological studies. Nowadays, ALD is considered one of the most promising techniques for nanoscale device development and fabrication.

Thin films are an unreplaceable part of any modern technology, concerning applications like surface coatings or nanoelectronics fabrications. Such films must be of high electronic and structure quality and usually require vapor-phase deposition techniques. The growth of polycrystalline and amorphous films began in the 1980s with methods as chemical vapor deposition (CVD) and physical vapor deposition (PVD). CVD is a technique involving chemical reactions. Two or more volatile chemicals called precursors decompose at the material's surface, leaving a thin film and byproducts. The material is usually referred to as a substrate and must be heated as the reactions are driven thermally.

These vapor phase epitaxy methods were improved over time into, e.g., metalorganic CVD (MOCVD) or molecular beam epitaxy (MBE). MOCVD, however, cannot deposit layers in the units of nanometers. MBE is a reliable thermal evaporation process where the grown film thickness can be controlled in real-time, yet it requires an ultra high vacuum environment, making it operationally inefficient.

ALD was invetned by Dr. Tuomo Suntola in 1970s in Finnland. At that time, the method was called atomic layer epitaxy and held the revolutionary idea of depositing crystalline materials one atomic layer at a time. It was mainly developed for the production of flat panel displays. The method caught interest in the late 1990s, when the deposition of metal oxides was cultivated and used in semiconductor research; the name ALD was established as well. Over the past years, the variety of ALD materials has significantly expanded, including also nitrides, carbides, and even organic materials.

The unique ALD properties come from the deposition process that is based on self-limiting chemical reactions of precursors and substrate, identifying ALD as a self-assembly technique. ALD procedures were partially developed from the known CVD processes, but the exposure of precursors was altered, leading to notable decreases in needed process temperature. ALD also offers exceptionally conformal thin film production, including thickness control at the atomic scale. Due to these benefits, ALD has become the first choice in many applications. It is able to fulfill the ever-growing requirements of the microelectronics industry, which other methods fail to meet.

This thesis is intended to introduce the reader to the basics of ALD and highlight selected applications, including high-κ gate dielectric transistors. The second part of the thesis is dedicated to an existing ALD system from the SENTECH company recently installed at the laboratory at FEE, CTU. Several experiments will be introduced as well in the experimental part, confirming the correct installation of the ALD system.

Chapter 2

Basics of Atomic Layer Deposition

A thin ALD film is built up in cycles. In each cycle, a submonolayer of material is deposited onto the surface of the substrate. In one cycle, the substrate is exposed to several precursor chemicals, each containing different elements of the final material.

Precursor chemicals are introduced to the reactor space separately, enabling them to react with the surface in a self-limiting way. In other words, the precursor molecules react with the surface chemical groups as long as these are available. This process will eventually lead to saturation, leaving the surface with a new uniform layer. This sequential exposure to precursors gives ALD its unique characteristic. It prevents uncontrolled and unwanted chemical reactions and byproducts and constructs the exceptionally conformal material layers.

2.1 A Typical ALD Cycle

A typical ALD cycle occurs in a vacuum reactor. As described in the schematics in Figure 2.1, one cycle consists of four steps: (1) the precursor exposure, where the precursor, a gaseous chemical with a metal compound, is pulsed into the reactor for a designated time, allowing it to fully react with the surface of the substrate. Next is (2) the purge period, where an inert carrier gas (usually N_2) flows through the reactors and removes any unreacted precursor or reaction by-products. This is followed by (3) exposure

to a second precursor, also referred to as co-reactant (usually oxidant). At this time, a monolayer of the desired film is formed on the surface. The ALD cycle is completed with the second (4) purge period.

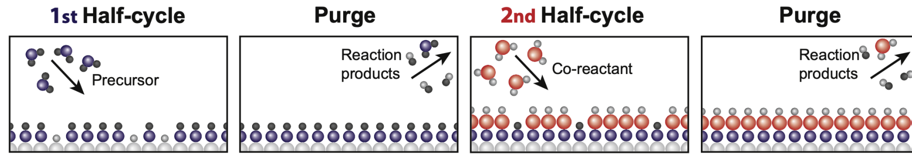

Figure 2.1: Schematics of one ALD cycle. [3]

The most widespread example of ALD is Al_2O_3 film fabrication. It is made with Trimethylamine (TMA) as the first precursor that leaves the surface covered with $AlCH_3$. As co-reactant, vapor H_2O is used. The total chemical equation of this process is

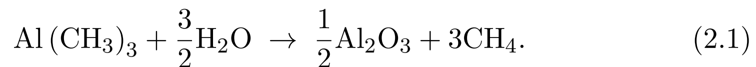

$$Al\left(CH_3\right)_3 + \frac{3}{2}H_2O \ \rightarrow \ \frac{1}{2}Al_2O_3 + 3CH_4. \tag{2.1}$$

The precursor and co-reactant chemicals must be chosen well as they have to react with the substrate but must not react with themselves or with the surface molecules they create (more on precursors in Chapter 2.3). The pulses of precursors must also be long enough to allow chemical reactions to saturate, leaving the whole surface covered. Reactions between precursor and co-reactant molecules are prevented by purge periods that do not leave such components on the material's surface or in the gas phase and are also timed.

This cycle is repeated until the desired film thickness is achieved. The typical growth per cycle (often referred to as GPC) rate is about 1 Å and the time range of one cycle goes from one to several seconds depending on the ALD system and process design. Note that some films can also be grown using three or even more precursors, creating a so-called supercycle with more than four steps leaving the product with a wider variety of films. It is even possible to create new artificial materials with unique features this way, making ALD a powerful technology for nanotechnology research.

In general, the process is conducted at temperatures lower than 350 °C and requires both the substrate and the reactor to be heated. The temperature range for which the correct ALD behavior is obtained is known as the temperature window. Temperatures outside the window lead to a poor growth rate and can altogether change the principle of deposition. Lower temperatures may cause condensation of precursors on the surface. They could also decrease the reactivity of molecules with the surface preventing reaction saturation and lowering GPC. High temperatures also bring unwelcomed

features such as decomposition of precursors, which leads to a CVD-like growth or desorption of the surface material and hence lower growth. In conclusion, the temperature window is a range where the GPC should be only slightly or not at all temperature-dependent. That is how the saturation of reactions together with the desirable ALD deposition is ensured.

2.2 Characteristics and Advantages of ALD

ALD's unique characteristics are based on the self-saturating surface-controlled film growth and the sequential process. Leading metrics are an excellent conformality of the film, followed by precise thickness control and altogether low deposition temperature.

Let us start with **conformality**, which is the main factor in choosing ALD over CVD and similar technologies. Conformality derives from the self-limiting adsorption of precursor. It enables highly uniform coatings over the surface of the substrate as well as equal thickness in 3D structures as trenches or pores. There are two main requirements to reach the even film thickness over such structures. It is a sufficient pulse time and molecule flux of precursors allowing them to reach all substrate areas. When such conditions are ensured, the ALD is able to cover even deep trenches evenly, as demonstrated in Figure 2.2, where the coating of semiconductor memory devices is shown. When working with complex nanostructures, the degree of saturation may differ on top and at the bottom of the substrate. Molecule flux decreases going to the bottom and may lead to incomplete saturation. Also, purging periods must be carefully timed to prevent CVD growth deeper in the structure.

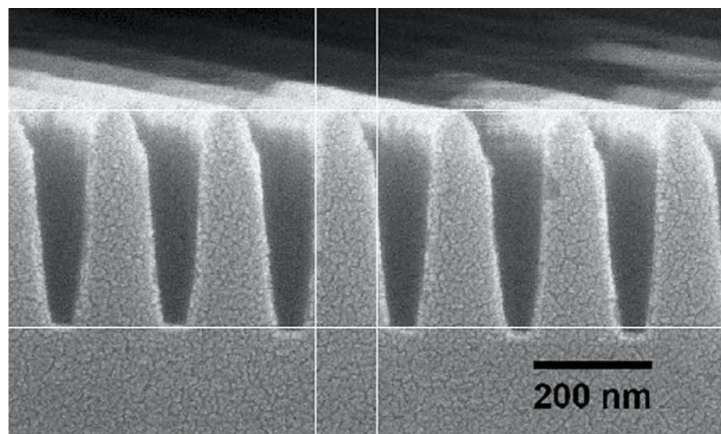

Figure 2.2: ALD coating of trenches. [2]

The self-limiting nature of ALD and the possibility of controlling the number of cycles enable the film's exact **thickness and composition control**. Moreover, considering this concept of layer-by-layer deposition, thickness control is available on the atomic level. Therefore ALD comes into play whenever an extra-thin film is needed, e.g., for capacitor insulators, gate oxides in MOSFETs, and many more, as described in Chapter 3. The continuous uniform growth also provides a pinhole-free coating which is another feature that all high-quality insulators need.

However, when controlling thickness on the atomic level, the final film measurement is usually not a direct sum of all the monolayers of the deposited material. For most ALD cases, the GPC is a bit smaller than the growth rate of a single monolayer. It is caused by the steric hindrance of molecules (larger parts of molecules hinder small molecules causing slow or no chemical reaction). It is possible to predict the growth rate based on the steric hindrance and the number density of molecular adsorption sites. Factors such as substrate materials and growth temperatures also affect the result. Another unpleasant phenomenon that must be considered is the formation of islands in the initial growth stages. This also affects the growth rate and causes non-linear growth of the film, preventing a smooth surface. Island formation is observed in some material systems, with metal deposition on oxide substrate being the frequent example.

Another characteristical advantage is the generally **low temperature** of the deposition process that still maintains its quality. Nevertheless, the chemical reactions must still be thermally controlled. Therefore heating of the substrate, the reactor, and the precursor tubes is necessary. For some materials, ALD can produce a relatively pure film at temperatures under 100 °C. The previous example of Al_2O_3 made with TMA and water is a model low-temperature process possible at 33 °C. Al_2O_3 deposition was even achieved at room temperature when replacing water with ozone, O_3. [4] The low-temperature deposition widens the substrate choices to materials with a low melting point, such as polymers. Plastic substrates might play a key role in the development of flexible electronic devices, e.g., flexible displays. Metal ALD usually requires higher growth temperature, partially because of a lower reactivity of the chemical process, and thus growth below 100 °C is rarely executed. One such rare example is a deposition of Pd at 80 °C using bis(hexafluoroacetylacetonato)palladium [$Pd(C_5HF_6O_2)_2$] and molecular hydrogen. [4] To lower the temperature more significantly, the Plasma Enhanced ALD (PEALD) was developed. This method utilizes plasma for better activation of reactants and will be more described in Chapter 2.4.

Before concluding this chapter, one more drawback of ALD must be mentioned. The layer-by-layer fabrication, the pulsing and purging periods, and

generally a long cycle time induce **slow deposition rates**. Most ALD rates range between 100-300 nm/h. [1] The reactor design and structure of the substrate play the primary role in the deposition time. Bigger volume of the reactor chamber and larger or more complicated shape of the substrate (e. g., trenches) lead to longer pulsing and purging periods. In order to suppress this drawback, a new method called Spatial ALD was developed and will be mentioned further below.

2.3 Precursors and Co-reactants

A wide selection of materials has been grown by ALD and reported in numerous studies. [1, 2, 3, 4] New materials and ALD processes are being actively developed as well. The research has taken a significant leap from the very first ALD demonstration in the mid-1970s, which used elemental zinc and sulfur to grow ZnS. In Table 2.1, an overview of all materials prepared by ALD that were known in 2019 is described and structurally written down into a periodic table. The most common types of precursors nowadays are oxides followed by nitrides, sulfides, and pure elements. The final product of ALD can be crystalline or amorphous and varies from metals and insulators to semiconductors. Materials deposited from three or more elements also gained interest, their properties winning over the complexity of the ALD process scheme (also called a supercycle). Some of the well-known compounds are $SrTiO_3$ or $HfSi_xO_y$. [3]

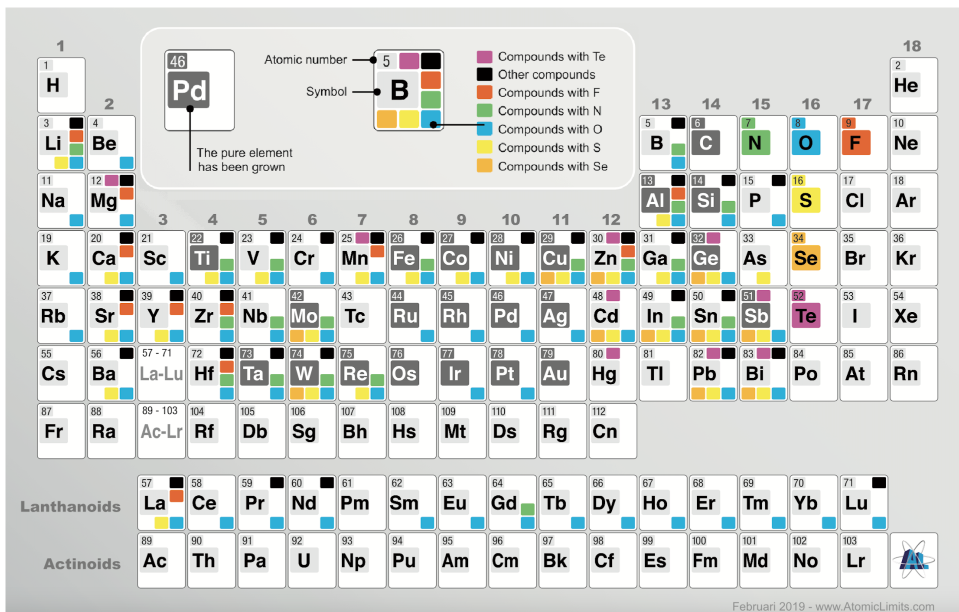

Table 2.1: Overview of the materials prepared by ALD. [5]

As mentioned before, there is a wide selection of ALD materials. However, it does not encompass all the materials, the main limitation being the unavailability of effective reaction pathways. In order to avoid uncontrollable reactions and maintain the self-limiting growth in the gas-phase process and overall stability, precursors must fulfill several requirements:

- sufficient volatility but no decomposition at the deposition temperature
- sufficient and preferably fast reactivity with the surface sites and towards the other precursor leading to growth saturation
- neither the reactants nor the reaction products should dissolve or damage the substrate, the reactor, or the growing film
- preferably low-toxicity and easy handling (liquids are ideal)

Finally, the material availability (or possible synthesis) and cost must be taken into account. Choosing the best precursor is not an easy task and usually consists of balancing more and less desired qualities together with economic possibilities.

The first precursor to be introduced to the reactor is usually a metal reactant. Metal precursors can be either inorganic: elemental, halides,... or organic: alkyls, amides, beta-diketonates,... Let us look at some benefits and drawbacks of a few groups from this extensive collection of materials. Halides such as $HfCl_4$ are very reactive, have high deposition rates, low steric hindrance, and are inexpensive. However, they have reactive by-products that may be incorporated into the film at low deposition temperatures. Furthermore, products such as HX (X being F, Cl, Br, I) may cause corrosion and etching of the film. Alkyls do not suffer from this problem, are still highly reactive, and can use H_2O as a co-reactant. They are not as well thermally stable, and their decomposition at higher temperatures is limited. Despite that, they are beneficial for the deposition of oxide materials, the previous example of Al_2O_3 being probably the most studied ALD precursor of all time. Another typical alkyl example is zinc and ZnO thin film. [2] Similar properties also have cyclopentadienyls. Even though they are available for only a small number of materials, they can be used for the production of integrated circuits, e.g., the production of HfO_2 by using $(C_5H_5)_2HfCl_2$. In general, for IC applications like HfO_2 or ZrO_2, metal precursors from halides and nitrates are more conventional. [4] The last group of precursors in this shortlist are β-diketonates. They are known for their volatility and good thermal stability and can be utilized for a wide range of elements. Unfortunately, their reactivity and growth rate are not very high, and they demand more reactive co-reactants as O_3.

The choice of the second precursor/co-reactant is also important and mirrors the features of the precursors above. Co-reactants are usually small molecules with good volatility and reactivity at a given temperature, adding a second component to the final film. The broadest range of co-reactants is related to metal oxides. The most commonly used ones are H_2O, O_3, O_2, N_2O_4, H_2O_2, and O^- from a plasma source. Out of this group, O_3 and O^- are the most reactive, enabling lower deposition temperatures. However, they are more prone to oxidize the substrate surface and creating an unwanted material layer. H_2O is more gentle towards the surface and is, despite its lower reactivity, most frequently applied. The deposition of pure metals is made possible mainly by H_2, though at a higher temperature. Zinc vapor, O_2, and more generally reducing agents were also successfully applied. [2, 1] This list of co-reactants shall be concluded with nitrides deposition. For a clean surface reaction, the deposition requires a nitride to be both the first precursor and co-reactant. In this way, NH_3 compounds must be used twice in the process to grow e. g. TiN or Ta_3N_5 thin film. [2]

2.4 Modified ALD Techniques

To fix some of the ALD shortcomings, various techniques were added to the basic ALD process. One of these modifications mentioned earlier in the text is the **Plasma-enhanced ALD (PEALD)**. This technique creates highly reactive co-reactants from a plasma source, the leading example being O_2 with H_2 and NH_3 in tow. The main advantage of PEALD is the capability to reduce the temperature range of a general ALD process and thus widely broaden the selection of precursors. However, the coating quality of vertical edges is lowered, and sometimes only one side of the substrate can be coated via PEALD.

Plasma-enhanced ALD can be sorted under a general modification called **Energy-enhanced ALD**, which also includes ozone-based ALD. [6] The main goal of this method is to obtain more reactivity by using species with short lifetimes. Such precursors must be produced in situ by applying a certain form of energy (electrical discharge, thermal cracking). Thanks to the short lifetime of reactants, long purge periods are not necessary. However, the precursors must be placed closer to the reactor chamber.

In Chapter 2.2, the disadvantage of slow deposition rates was mentioned, especially for the coating of complex 3D structures. To improve this drawback, **Spatial ALD** was introduced. Spatial ALD does not separate the steps of an ALD cycle in the time domain but instead in space. A spatially resolved

head is placed into the reactor and creates several reaction zones. Exposure to precursors can occur in different areas that are separated by purging gasses. Such deposition can happen when the head moves around the substrate, or the substrate moves past stationary precursor nozzles. Overall such spatial techniques increase the deposition rate to 3600 nm/h.

Another interesting modification is **Area-selective ALD** which, as the name suggests, is a deposition of a film at specific locations of the substrate. This selective process needs to begin with either deactivation of the unwanted area or activation of the area where the film will be deposited. Photolithography or etching are used for this and are followed up by the precursor adsorption on the chosen growth area. It is, however, quite challenging to obtain high selectivity due to imperfect growth initiation with minor defects and impurities. [7]

Chapter 3

ALD Applications

The main applications of ALD lie in the microelectronics industry. From semiconductors and memory devices to solar cells and energy storage, everything takes advantage of the conformal, pinhole-free, thickness-controlling deposition. The very first breakthrough in ALD manufacturing dates back to the mid-1980s. It was not surprisingly in Finland, where the production of TFEL displays begun and continued for over 20 years. [2] The research on ALD utilization in semiconductors development started in the 1990s as a potential new method that could possibly guarantee Moore's law conservation in the future. Especially when the industry started focusing on the use of high-κ dielectrics as a transistor gate oxide, the remarkable traits of ALD increased the technology demand. In 2007, Intel introduced ALD into their mass production in order to reduce transistor gate oxide thickness. [1]

Before some of the more specific microelectronics applications will be introduced, it must be mentioned that the ALD also reaches beyond electronic devices. The silver jewelry industry uses ALD coatings as a way of preventing the tarnishing of silver products. The coatings also have anti-corrosion and even decorative purposes on collector coins and in watchmaking. An ALD bioactive layer found a role in medical implants like dental joints or surgical fixators. [15]

3.1 FinFETs and high mobility FETs

The reduction of the gate oxide thickness in transistor development, although desirable for down-scaling of the devices, brought new performance limitations. Hence a search for more innovative alternatives to the traditional transistor concept began. The planar structure was changed in order to increase the transistor channel area covered by the gate oxide. Instead of a planar form, the semiconductor channel partially protrudes from the bulk crystal, forming a fin that is rising over the rest of the surface, as shown in Figure 3.1. This irregular structure naturally needed to be covered with a gate oxide of excellent conformity and without pinholes. This task appeared to be made for ALD and definitely owes its wide production to the existence of such a technique.

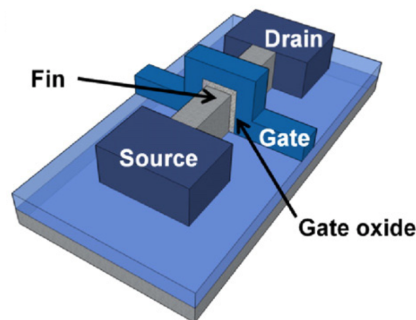

Figure 3.1: Schematic drawing of FinFET. [4]

Many more new generations of FinFETs are being researched. The main idea is to spread the gate oxide to encompass even more of the semiconductor surface. One variant is modeling the gate oxide into an omega shape, undercutting the gate a bit on the fourths side. Another version is called a Pi-gate, which covers the fin even below the surface.

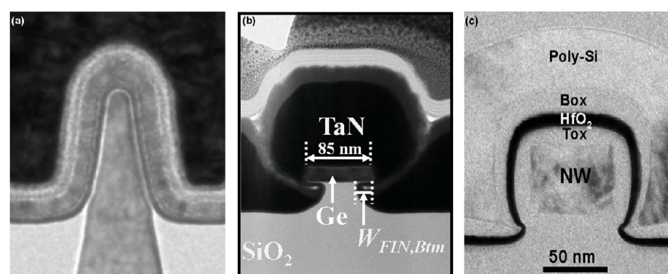

Figure 3.2: Different gate design structures with the use of ALD. (a) FinFET transistor, (b) Omega-gate structure wrapping around a Ge channel, (c) Pi-gate surrounding a Si nanowire. [1]

Another approach to balance the down-scaling limitations with the performance efficiency is to use high mobility channel materials instead of silicon. The increase in the electron and hole mobility leads to an increase in the devices' speed and power reduction; the saturation current is also improved. A good example of such material is III-V compound semiconductors with GaAs taking the lead with excellent electron mobility. On the other side, Ge is a material with outstanding hole mobility. These materials offer exciting possibilities, however, a high-κ dielectric is required to adapt to these materials, and that is the challenging part of the process.

Successful deposition of Al_2O_3 and HfO_2 for Ge was reported. [1, 4] A critical part of the coating is a good passivation layer on top of the Ge prior to the ALD oxide growth. The interface is rid of the native surface oxides, and the electrical characteristics of the gate oxide are visibly improved. The fabrication of GaAs MOSFET also proved to be difficult, mainly due to the poor electrical properties of the GaAs-oxide transition. It was a TMA and water deposition of Al_2O_3 as a gate oxide that brought good quality results at last. Another ALD material, HfO_2 from $HfCl_4$ and water, was successfully applied as a gate oxide to the GaAs device. [8] The study of ALD high-κ dielectrics continues for a GaAs channel, still electrical properties comparable to Si MOSFET are yet to be determined.

3.2 Non-volatile Memory (NVM) Devices

One of the more traditional ALD applications after gate oxides is in the field of dynamic random access memory (DRAM) devices. [3] The main development trends changed over time from down-scaling to low operating voltage, high speed, and non-volatility. The DRAM might be replaced by new memory devices, including nanocrystal (NC) memory, resistive switching memory (ReRAm), and phase-change memory (PRAM).

The NC memory is the most promising candidate out of the three mentioned variants. The nanocrystal memory is more scalable and operates under lower voltage than conventional memory devices. For a correct implementation, high interface quality and good tunneling oxide are expected. Again, high-κ materials are preferred over SiO_2, leading to improving charge loss properties due to a smaller electron barrier height. ALD can be used for a fine and reliable deposition of the tunneling oxide.

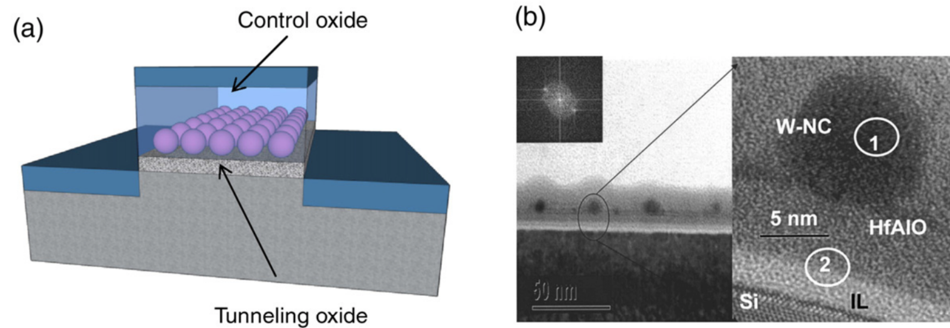

Figure 3.3: (a) Schematic drawing of NC memory and (b) TEM image of HfAlO/W/HfAlO structure of NCs embedded in HfAlO. [4]

One of the first ALD depositions used HfALO grown by $HfCl_4$ and H_2O as a tunneling oxide for the NC memory. [4] More variants were explored, generally leading to good performance with a data retention window of 0.7 V for 10 years. NC with a large memory window over 3 V were obtained for ALD deposition of ZrO_2 as well. These ALD grown oxides were compared with the SiO_2, showing higher charge tunneling probabilities and thus higher stored charge density. [9]

The future of ALD shows promise for applications in emerging electronics where the utilization of ALD is swiftly expanding. It plays a key role in the fabrication of lower dimensionality semiconductors with unique shapes like tubes or wires and structures like graphene or carbon nanotubes. The ALD oxide coating does not significantly disrupt even sophisticated materials properties. The precise thickness control on nano-scale and the excellent uniformity, together with other characteristics, secure ALD technology as a critical tool for nanotechnology and microelectronics research and development.

Chapter 4

SENTECH SI PEALD LL System

SENTECH Instruments GmbH is a German private company located in Berlin that engages in business fields like Thin Film Metrology, Plasma Process Technology, and Atomic Layer Deposition. [10] The company manufactures a wide range of respective systems. Leading the low temperature deposition branch is Inductively coupled plasma enhanced chemical deposition (ICPECVD) and Plasma-enhanced atomic layer deposition (PEALD). The ALD machine that will be presented in this chapter and later used in the experimental part is SENTECHS's SI ALD LL.

4.1 Brief View on ALD Market

The ALD systems are developed and manufactured by companies worldwide with perhaps a higher density in the USA. Two ALD systems commonly mentioned in ALD experimental articles are the PICOSUN ALD system and Veeco (Cambridge Nanotech) Fiji series. PICOSUN is a company from Finnland, the origin land of ALD, with a solid and historical position on the market providing ALD systems for both research and mass production. The American Fiji ALD is mostly research-oriented, similarly to Sentech, which is designed for research and small-scale production.

All three companies offer a plasma-enhanced variant of their ALD systems. The temperature range of the substrate processing is also relatively similar. SENTECH offers a 50 - 400 °C range with an optional variant up to 600 °C.

[12] PICOSUN can perform between 50 - 500 °C (650 °C optional). [17] And Fiji (with no lower boundary presented) is able to go from standard 500 °C up to 800 °C if desired. [18] Regarding the number of precursors, the differences are slightly bigger. Picosun has 6 separate precursor inlets enabling up to 12 different precursors sources. Fiji offers 4 - 6 separate inlets while SENTECH, though also capable of having 6 different precursors, presents only 4 inlets (but has up to 7 gas lines). These numbers are not as much evidence of the machine quality but more of a way to more widely cover the market's demand. All of the systems are able to work with liquid, solid, and gas precursors as well as with ozone.

A more vital factor is, however, deposition uniformity. The wide variety of ALD processes was in this thesis already stressed enough that it must be clear to the reader now that uniformity of deposition alters for different materials and dosing times. Yet, it seems that a standard metric is used, and it is the 1σ uniformity of Al_2O_3 deposition. PICOSUN presses down thermal deposition non-uniformities to only 0.13 %, [15] SENTECH closely follows with 0.15 % thermal and 0.58 % plasma deposition. [10] Fiji performs both thermal and plasma deposition with a defect of 1.5 %. [18] SENTECH's performance will be more thoroughly described in the next section. Let it be noted for now that it can clearly keep up with the top-of-the-market ALD systems. Before a price-wise point of view, the comparison will be finished with a slight mention of additional options that companies offer with their systems. Both SENTECH and Fiji present themselves as suitable candidates for research applications. It is not surprising then that both of them offer a variety of deposition observation and measuring techniques, namely Ellipsometry, Mass Spectrometer, or Quartz Crystal Microbalance, which can usually confirm the quality of the sample in-situ. PICOSUN (also containing in-situ analytics) focuses more on the up-to-date coating of complex 3D structures [16] and offers a diffusion enhancer, improving the deposition of deep trenches or porous structures.

For a price comparison, public data from several Czech universities were used. PICOSUN ALD system is steadily more expensive than others; the basic version costs around 12 million CZK. The Veeco Fiji system ranges between 6 (basic) - 11 million (advanced) CZK, only slightly higher or equal to SENTECH. The prices elevate with additional options like plasma equipment, heaters, in-situ analytics, or glovebox. In the end, SENTECH was chosen by the CTU's Faculty of Electrical Engineering due to a good experience between the German company and another company overseeing the construction of the new laboratory, where the ALD was supposed to operate. The total sum was around 10.5 million CZK, including all components of the ALD system.

4.2 SENTECH's ALD Performance

Before a more thorough description of the machine, its hardware and software, system performance will be shown in several figures. It will again be demonstrated on Al_2O_3 films deposited on 200 mm wafer from TMA and H_2O by thermal ALD and TMA and O_2 plasma by PEALD. Beginning with thermal deposition, Figure 4.1 (a) shows a graph of layer thickness quality. The grown layer was 49.9 nm thick and reported only 1.2 % error. Figure 4.1 (b) examines the film's uniformity using refractive index statistics and leads to the previously mentioned 0.15 % non-uniformity. The substrate temperature was 200 °C, and the growth rate was 0.8 Å/cycle with a duration of 2 s/cycle.

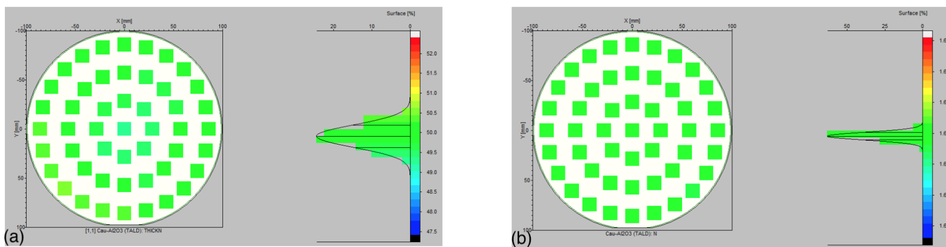

Figure 4.1: Properties of thermal ALD (a) layer thickness, (b) refractive index uniformity. [10]

Plasma-enhanced growth is captured in Figure 4.2. Graph (a) on the left reports again layer thickness quality. The grown layer was 26.8 nm thick and reported a slightly higher error of 1.6 %. Figure 4.2 (b) shows that non-uniformity has also increased in this case to 0.58 %. The substrate temperature was 200 °C, and the growth rate was 1.1 Å/cycle with a duration of 10.5 s/cycle. Although PEALD might seem weaker now due to this lower performance, its possibilities for broader film and precursor selection still prevails.

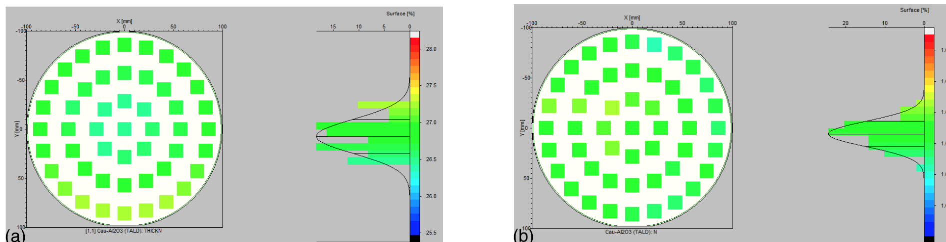

Figure 4.2: Properties of PEALD (a) layer thickness, (b) refractive index uniformity. [10]

The film thickness of both thermal and plasma-enhanced processes shows a linear dependence on the number of cycles, as seen in Figure 4.3. It can also

be observed that PEALD indeed has a higher growth rate over thermal ALD. Overall, SENTECH presents its ALD as a flexible system build for a wide range of processes with very good uniformity and conformality that can be further optimized by in-situ analysis.

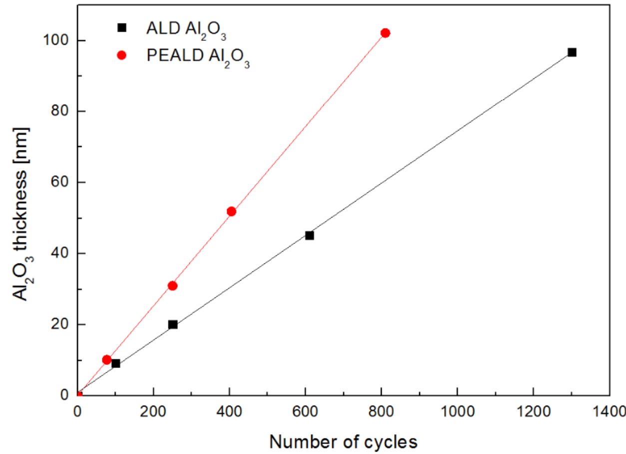

Figure 4.3: Linearity of growth. [10]

4.3 SI PEALD LL Description

As mentioned before, SENTECH's ALD is designed for research, use in universities, and small-scale production. Hence it can provide a wide range of deposition modes using flexible system architecture. The deposition of oxides, nitrides, metals, and other materials is possible by thermal and plasma-enhanced processes. The plasma source is included in the upgraded PEALD model, and the system can be additionally expanded with in-situ monitoring called Real Time Monitor, with additional precursor lines and other options. The system can be separated into the following modules:

- Reactor unit containing reactor, load lock, and electronics
- Gas and precursor cabinet and supply system
- Computer with SENTECH software
- Real Time Monitor
- Pumping system
- Mains connection box

Figure 4.4: SI PEALD LL system. [10]

In the standard deposition process, all chambers are under vacuum. This vacuum is maintained utilizing foreline and turbo molecular load lock pumps. The function of the **pumping system** is vital in the handling of the wafer, which is conducted between pumped chambres, and for removal of possible dangerous gasses. For better integration of the sample into the ALD loading chamber, an external glovebox can be used. The wafer handling needs to be done manually before using the automatic load lock. The glovebox workstation filled with nitrogen ensures that this process is done in an inert atmosphere and later protects the newly growth film.

The **mains connection box** contains a power supply unit that distributes electrical power within the ALD system. The front panel of this box also includes the main switch button, other buttons and light indicators, and coded sockets for components, e. g. pumps. The rest of the modules will be introduced in separate sections as they deserve more space for a proper description.

4.3.1 Reactor Unit

The heart of the reactor unit is an inner cylindrical process chamber. This chamber is made from a monolithic, seamless ingot, ensuring low leakage. The chamber is built out of aluminum AlMgSi and has additional flanges: upper flange for plasma source, side flange for load lock, optional flanges for in-situ monitoring, and bottom flange for the vacuum system. A substrate electrode is located in this cell. The stainless steel electrode is equipped with an integrated heater and thermocouple sensor. The main goal of the electrode is the heating the substrate material (also called a wafer). This wafer can have a diameter of up to 200 mm and is carried on a substrate plate with 220 mm diameter. The electrode can heat the material from anywhere between 50 to 400 °C (500 °C optional). Reactor wall temperature can be set up to 150 °C. However, with the additional isolation for plasma source and with Real Time Monitor, the maximum temperature drops to 100 °C.

Single wafers are loaded into the reactor via a vacuum load lock. The load lock is made from the same material as the reaction chamber, has a transparent lid and a pick-and-place mechanism which enables clean and careful handling of the substrate. It is connected to the reactor by a rectangular gate valve 32 x 222 mm. The automatic (un)loading is done by a pneumatic transfer mechanism, and part of the process is also an evacuation of containing gas and a purge with nitrogen. The load lock works under base pressure lower than 10^{-1} mbar and has a maximum leakage rate 10^{-3} mbar·l/s.

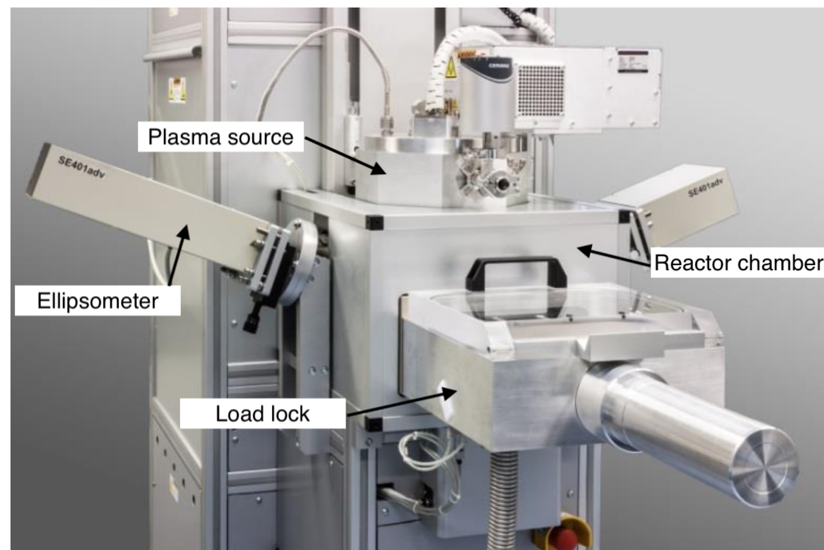

Figure 4.5: SI PEALD LL Reactor unit with RTM. [11]

All the vacuum needed for the correct system process is supplied by the vacuum system. It is equipped with a dry roots pump resistant against

corrosive gases. It is also water-cooled, nitrogen purged, carries several sensors and control features, and overall provides reliable pressure operation. The safety of the operator is moreover ensured by the programmable features of the reactor unit. In both the load lock and the reactor, purging cycles are set via system software and, besides the secured safety, contributes to chamber cleanliness.

4.3.2 Precursor and Gas Cabinet

The precursor and gas cabinet contains different precursor pots, precursor lines with several cut-off valves in their way, and mass flow controllers (MFCs). MFCs control all gas lines, purge/carrier gases as well as a plasma source, and provide highly constant flow rates. Moreover, they are equipped with particle filters. Up to three MFCs can be provided for precursor delivery. The control values of the MFCs are set accordingly to the ALD process and can be altered from the user interface.

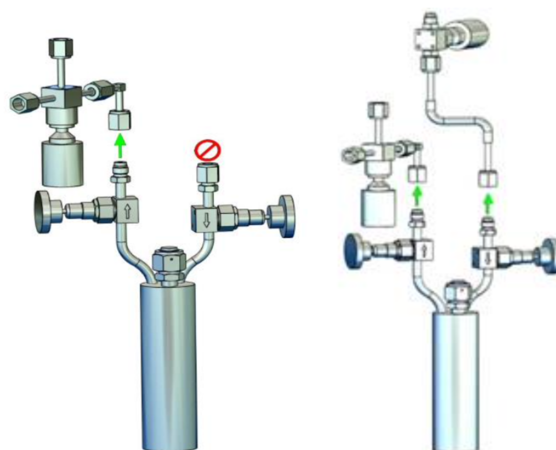

Figure 4.6: Direct draw (left) and bubble draw (right) precursor containers and their installation. [13]

There are two different methods for the delivery of precursors with different properties into the reactor. A direct draw is used for chemicals with high vapor pressure; for low vapor pressure chemicals, a bubbling draw is utilized. The precursors are supplied in cylinders or bubblers fitted with one or two manual valves, respectively. These containers' sizes can vary from 50 to 600 ml, with the standard pot being a 300 ml stainless steel bubbler from STREM Chemicals. Pots are attached to the precursor line and can be optionally equipped with heating devices. The standard offer includes 4 precursor lines with separate inputs into the reactor installed in the precursor magazine. Two more precursors can be added however they are added into a series

with a shared line into the reactor. The lines are made from electro-polished stainless steel with a 6 mm diameter. All lines are separately heated (up to 200 °C) and connected to the lid of the reaction chamber.

The plasma source, or more accurately capacitive coupled plasma source (CCP), is attached to the upper flange of the reactor. This remote source is driven by a 13.56 MHz generator and uses an external box for the 50 Ohm output impedance of the generator to match the plasma load. The power supply equals 300 W, and the pressure range of the cell is 0.07 - 1 mbar. The CCP source verges on a gas line (with MFC); another 4 non-corrosive gas lines can be added if desired. The gas line leads to the reactor chamber, where the high flux of reactive gas species is provided at the substrate surface.

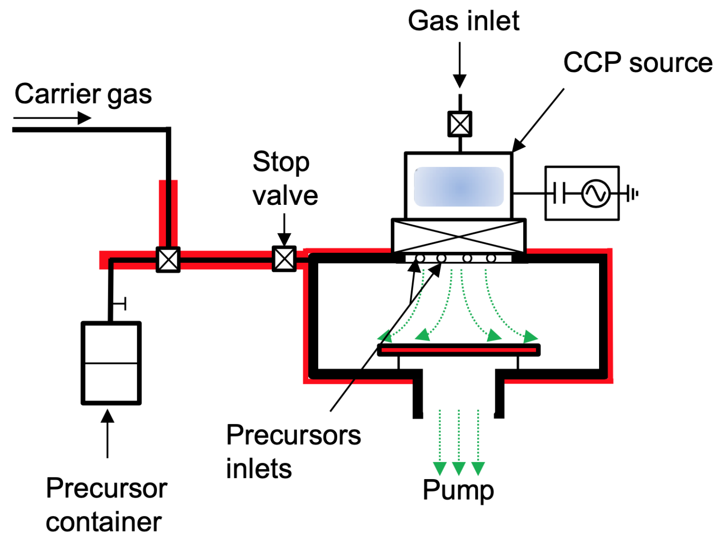

Figure 4.7: Reactor chamber and plasma source schematics. [11]

4.3.3 Hardware and Software Control

The system is controlled by hardware and software architecture. A reliable remote field controller (RFC) secures basic safety interlocks and enables real-time control of all components. This control is done via the serial field bus; bus nodes are located in the control rack and the reactor unit. The architecture enables quick manipulation with components and error diagnostics while being noise-immune, fast, and with a stable, experienced protocol. Additional Windows PC is supplied and used for process control, better visualization, and advanced data logging. The PC communicates with the RFC by Ethernet and is also equipped for LAN communication with the clients.

The SENTECH software offers a user-friendly interface that enables comfortable process development by writing recipes and the following monitoring in an ALD process. Here, RFC provides additional safety control, independent of the software for jeopardizing error commands or input data. The deposition process can be done manually or automatically via a recipe. The recipe mode is produced from a predefined sequence of steps that are performed automatically. Moreover, operations like opening the precursor lines can only be done automatically, as the movement must be swift. The program further allows the operator to control other command executions like opening the dry pump's valves or setting reactor and precursors' temperature. Graphical data logging is displayed together with the current state of the system. The software employs a device called a sequencer for the organization of ALD cycles. The sequencer is able to call up hardware components like valves and MFCs within one cycle. Accordingly to chosen time intervals, it controls flow rates of chemicals with a minimal time step of 10 ms and repeats the cycles as defined in the recipe.

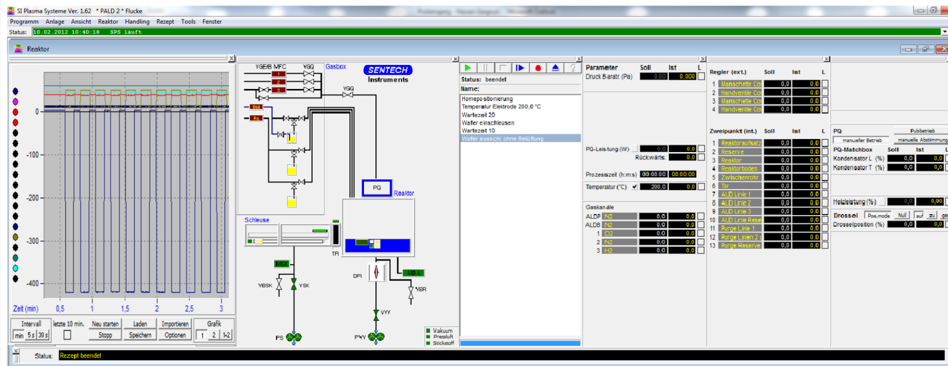

Figure 4.8: ALD system software example. [10]

4.3.4 Real Time Monitor

Real Time Monitor (RTM) can monitor each step within a single ALD cycle and measure the thickness changes between deposited layers, all in-situ with real-time values. The analysis can be done with different methods: mass spectroscopy, quartz crystal microbalance. However, the most desirable methods used are optical methods like ellipsometry as they do not influence the ALD process, are surface sensitive, and fast. The principle of the ellipsometer is captured in Figure 4.9. and its real implementation in Figure 4.5.

The key factor in ellipsometry is a measurement change of polarization upon reflection of the incident radiation after it interacted with the material.

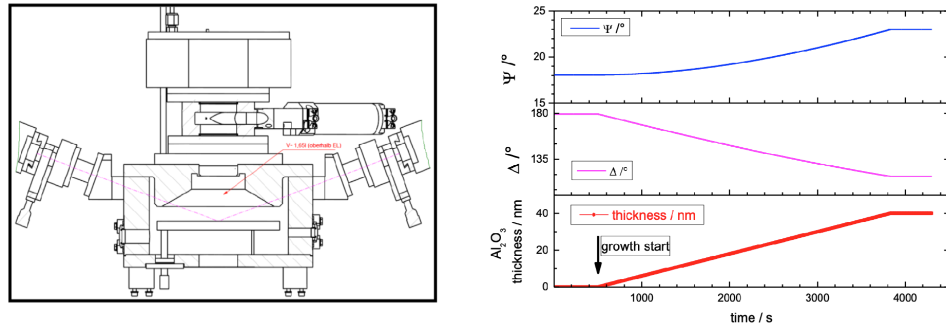

Figure 4.9: PEALD with ellipsometer and the principle of ellipsometry analysis. [10]

The polarization change is quantified by the amplitude ratio Ψ and the phase difference Δ. [14] The reflected signal depends on the material properties, like refractive index, and their measurement can be transferred to thickness (see Figure 4.9). Furthermore, the data are able to determine precursor pulse, co-reactant pulse, and purge times in between. The ALD growth and saturation can be consequently observed in every cycle.

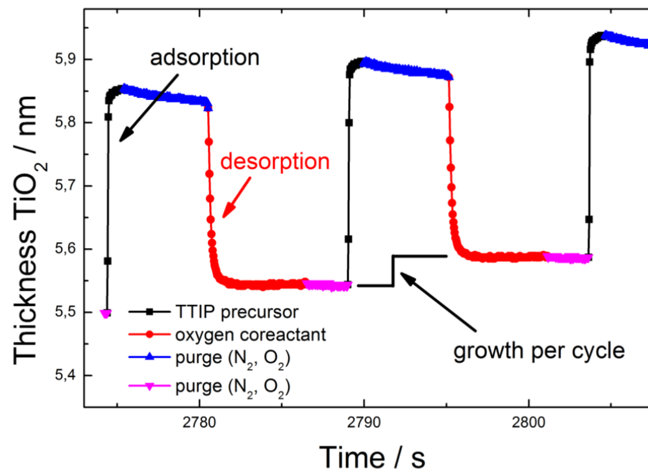

Figure 4.10: Real time monitoring of TiO_2 deposition. [11]

Thanks to the RTM dynamic substrate monitoring, a deeper understanding of surface reaction can be gained as well as better optimization of the ALD process by saving purging and dosing time and precursor consumption. RTM has its own software that communicates with the ALD software and contributes to the confirmation of a correct ALD regime.

Chapter 5

Experimental Part

The experimental part of this thesis is dedicated to the SENTECH SI PEALD LL system that was recently bought by the Faculty of Electrical Engineering, CTU. The machine is stationed in a new laboratory operated by the Department of Microelectronics. In this chapter, the very first steps of the ALD machine are captured. First, there will be a brief description of the ordered SENTECH ALD system, followed by its first trial deposition of Al_2O_3 and SiO_2 thin films on Si wafer. The samples will be examined by AFM and Raman spectroscopy. These methods will be described here as well, with a short theoretical resume in the beginning. Finally, an experiment involving a capacitor with a dielectric layer of PEALD grown Al_2O_3 will be introduced.

The ALD system purchased by CTU is plasma-enhanced with RTM corresponding to the description in Chapter 4. Additionally, a glovebox from MBRAUN was installed together with a CLEANSORB scrubber (CS Clean Solution) for the adsorption of waste gases. There is a photo of the system installed in the laboratory in Figures 5.1 and 5.2. Figure 5.2 shows a side view of PEALD with open precursors and MFCs cabinets.

5.1 Preparation

The initialization of SI PEALD LL is fairly straightforward. The machine and RTM must be switched on manually, but after that, they are accessible via the supplied software. After ensuring that all pumps and the scrubber are

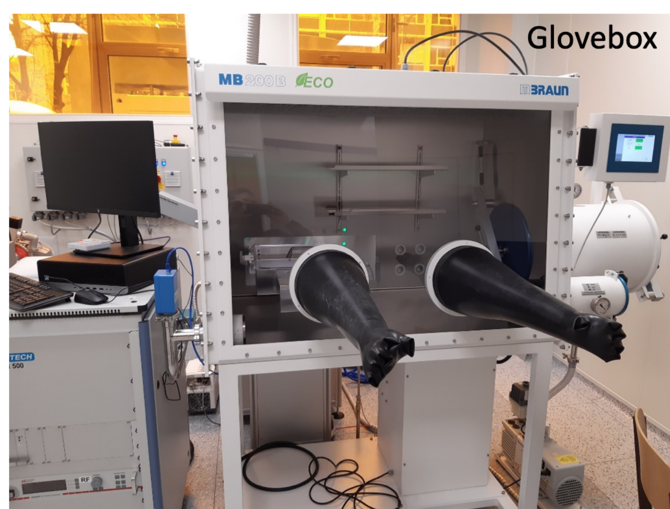

Figure 5.1: Front view of the glovebox connected to PEALD. [2]

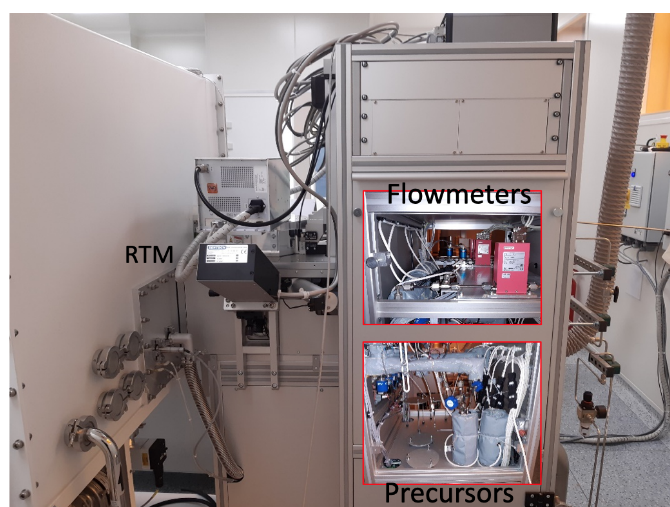

Figure 5.2: Side view of PEALD. [2]

in running mode, the operator can open valves via the software, connecting them with the system. Manual calibration of the ellipsometer is also needed and is done with support from the RTM software.

With the ALD system running, several checks need to be done before the first deposition and after a certain amount of time as part of the maintenance cycle of the machine. One of the important tests is the water test for nitrogen (N_2). Nitrogen is the main carrier gas of the system, enabling precursors dosing and purging. The amount of water in the gas needs to be checked, and the correct flow rate of the gas ensured. When a new precursor is installed, a protocol must be run to equilibrate pressure in the reactor chamber, the precursor line, and the container. This is usually done by repeated opening

of respective valves until there are no pressure peaks observed. Before the deposition, it is also desirable to activate the plasma source and adequately heat the system. Specifically, to heat the reactor chamber, the precursor containers, and the dosing and purging lines. After inserting the substrate from the load lock to the reactor chamber, enough time must be given for the substrate electrode to heat the sample, as this is usually the highest temperature component in the system.

5.2 Trial PEALD Growth of Thin Oxide Layers

Having the PEALD system running and prepared as written above, the deposition process could begin. A silicon wafer (with diameter of 100 ± 0.5 mm) was chosen as a substrate and placed into the reactor via the glove box and load lock. For the Al_2O_3 thin film, TMA was used as a precursor; for the SiO_2, the precursor was a chemical called SAM24, bis(dimetylamino)silane. Both processes used O_2 plasma with 200 W power as a co-reactant and nitrogen with a flow rate of 40 SCCM as a purge gas. The substrate was in both cases heated to 200 °C, TMA precursor was utilized via a direct draw, whereas SAM24 needed a bubble draw, with bubbler at 60 °C. The PEALD cycle was designed by SENTECH, which supplied the appropriate recipe. The recipe was loaded into the software platform, and the RTM was synchronized, monitoring the growing film thickness. Table 5.1 shows the time of each step of the PEALD cycle defined by the recipes.

	Al_2O_3	SiO_2
Precursor	0.06 s	0.2 s
Purge	2 s	4 s
Plasma	3 s	1 s
Purge	5 s	5 s

Table 5.1: PEALD dosing and waiting times

The Al_2O_3 film was grown into a 70 nm thick layer, the SiO2 film into 50 nm. The deposition went through successfully with no in-between system errors. The samples were then evacuated from the reactor, and after cooling down, subjected to the Raman spectroscopy and AFM.

5.3 Characterization Methods

5.3.1 Raman Spectroscopy

Raman Spectroscopy is a molecular spectroscopy technique that uses the interaction of light with matter to gather chemical and structural information. Observed light scattering is used for the measurement of molecular vibration of the surface and the interior of the sample. Collected data can then be formed into molecular (Raman) 'fingerprint', and used to identify a substance.

The key factor of this spectroscopy method is Raman scattering. When light interacts with molecules in a material, most photons are scattered at the same energy as the incident photons (described as Rayleigh scattering). But in a rare event, Raman scattering occurs when a small number of these photons (1 in a 10 million [20]) will scatter at a different frequency. The difference between the energy of the incident photon and the scattered photon is called the Raman shift. With these data, a Raman spectrum is rendered. The shape of an observed Raman spectrum is then compared to spectrums of known materials, and the measurement result is concluded.

Raman spectrometer used in the experiment is the inVia Qontor from Renishaw (Figure 5.3). The system offers three lasers with wavelengths of 532 nm, 633 nm, 830 nm; and has additional options like conducting an averaged spectrum from a large number of measurements.

Figure 5.3: (a) Renishaw's Raman spectrometer [22], (b) NTEGRA atomic force microscopy device. [25]

5.3.2 Atomic Force Microscopy

Atomic force microscopy is a technique that enables imaging of almost any type of surface profile (semi/conductors, polymers, ceramics, etc.). It consists of a sharp tip with a diameter from 10 to 20 nm attached to a cantilever, both usually made from Si or Si_3N_4. [23] The tip is scanned over the surface, interacting with it and using a feedback loop to adjust parameters for better imaging and tip protection. The tip-sample reactions are mapped with a laser beam deflection system (Figure 5.3), and with this, many force interactions can be measured: wan der Waalse, electrical, magnetical, etc.

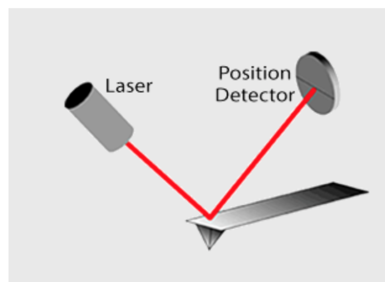

Figure 5.4: Laser beam deflection for AFM. [2]

The AFM has two basic operation modes. In the contact mode, the tip is in continuous contact with the surface. This mode is used for a lesser amount of applications than other modes. The tapping mode and the semi-contact mode both offer a different approach: The cantilever carrying the tip is vibrated above the sample surface in such a way that the tip comes into contact with the surface intermittently. By moving the tip across the sample, the atom at the apex of the tip reacts with individual atoms on the surface and forms chemical bonds with them. These interactions slightly alter the vibration frequency of the tip, which is detected via the laser beam.

Hence, the AFM can provide a 3D surface profile with almost zero sample preparation requirements and under ambient atmosphere. However, the scanning of the surface is sensitive to higher surrounding vibrations, and the microscope must be placed on sufficient vibration isolation (e.g., marble base). The AFM device used in the experiment is NTEGRA by NT-MDT Spectrum Instruments (Figure 5.4).

5.4 Results and Discussion

The human eye can not distinguish the 70 nm and 50 nm layers of Al_2O_3 and SiO_2, neither was a change of the surface structure observed. However, what could have been seen after the deposition process was a slight change of the wafers' colors. The original silicon wafer was silver, Al_2O_3 colored the substrate with dark blue, and the SiO_2 substrate had a brownish reflection.

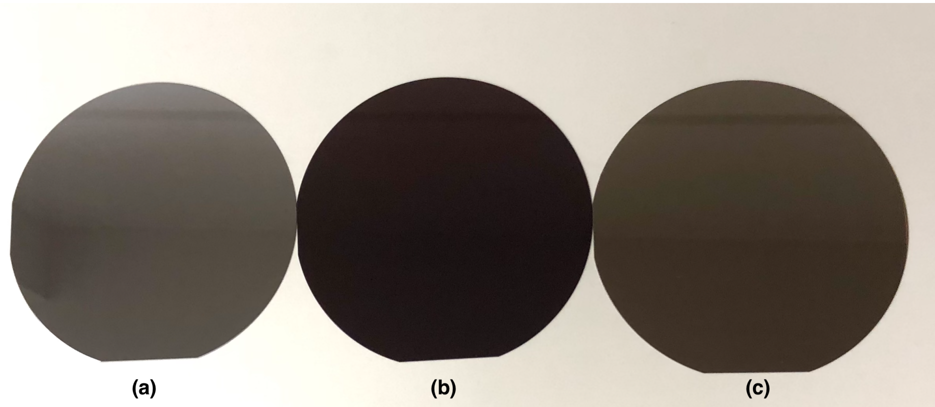

Figure 5.5: (a) original Si wafer, (b) wafer with Al_2O_3 thin film (c) wafer with SiO_2 thin film.

Both samples were examined by Raman spectroscopy. Raman spectrums were measured with all three lasers with almost identical results. For picture representation, a laser that measured the 'nicest' spectrum (smoothest, slightest noise) was usually chosen. However, since the thin layer of oxide is practically negligible in the mass of silicon, the Raman spectroscopy did not recognize the deposited layers. Some scientific articles admit that, e.g., the Al_2O_3 layer does not exhibit Raman signal [28] and use this method only to compare the intensity of the spectrum for films with different thicknesses. But according to [27], slight peaks at 428 cm^{-1}, 613 cm^{-1}, and 665 cm^{-1} can be assigned to the oxide material. Those peaks could have been only very slightly seen after the data were rid of the main peak. The original Raman spectrum of Al_2O_3 is in Figure 5.6 and is also almost identical to the SiO_2 spectrum. For comparison, the Raman spectrum of plain Si wafer is also shown (Figure 5.7); consequently, the overall difference in amplitude can be observed. In conclusion, Raman spectroscopy verified that the samples were unperturbed, and no damage was done to them.

The analysis by atomic force microscopy demonstrated the quality of the grown thin films better. By imaging the sample in semi-contact mode, a measurement of the surface was taken and graphically illustrated. Figure 5.8 is dedicated to the Al_2O_3 layer. The diagram on the left represents the original measurement in planar form. A gradual but smooth change in

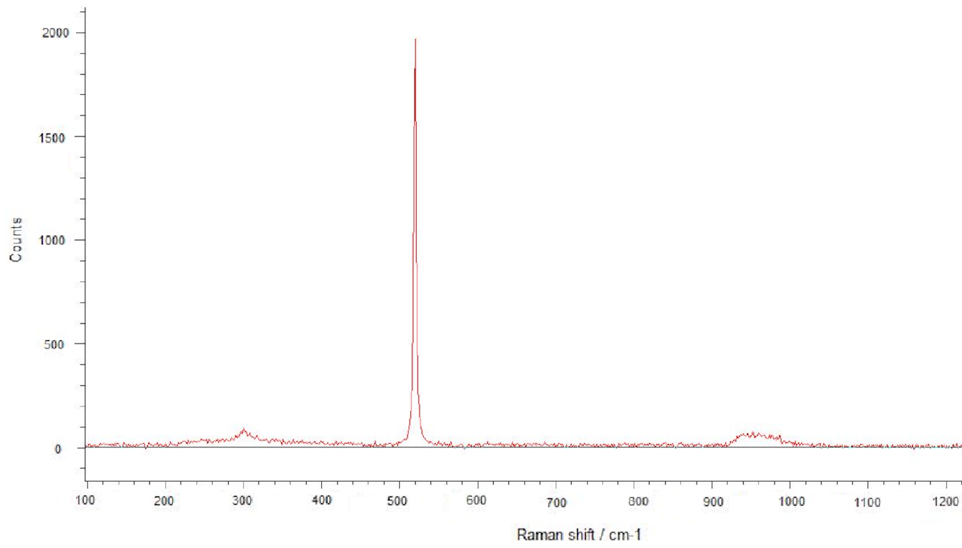

Figure 5.6: Raman spectrum of Al_2O_3 film measured with 633 nm laser.

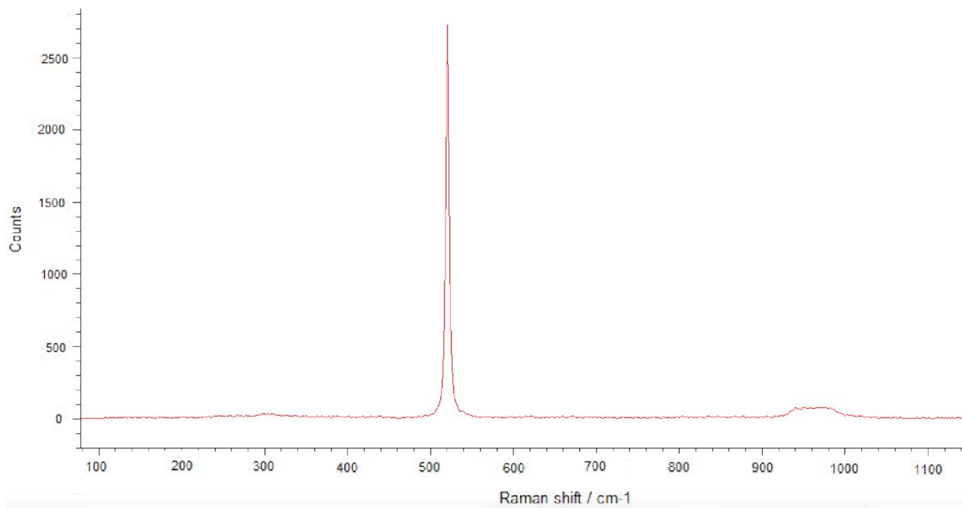

Figure 5.7: Raman spectrum of plain Si wafer measured with 532 nm laser.

height can be observed, with a maximum difference of about 100 nm. This continuous disproportion can only mean that the sample was tilted during the measurement. In Figure 5.8 (b) there are the same data as in figure (a), but flattened by the AFM software and hence devoided of the undesirable tilting. They are for better visualization modeled in 3D graphics. A fairly smooth surface is displayed with only a 2 nm difference at most.

The AFM measurement of SiO_2 was evaluated analogically to Al_2O_3. Figure 5.9 (a) shows again a continuous change in height with a maximum variation of 50 nm. The flattened 3D graphics reports a surface inequality that is not higher than 0.8 nm. Figure 5.9 (b) also shows that surface is corrugated in a

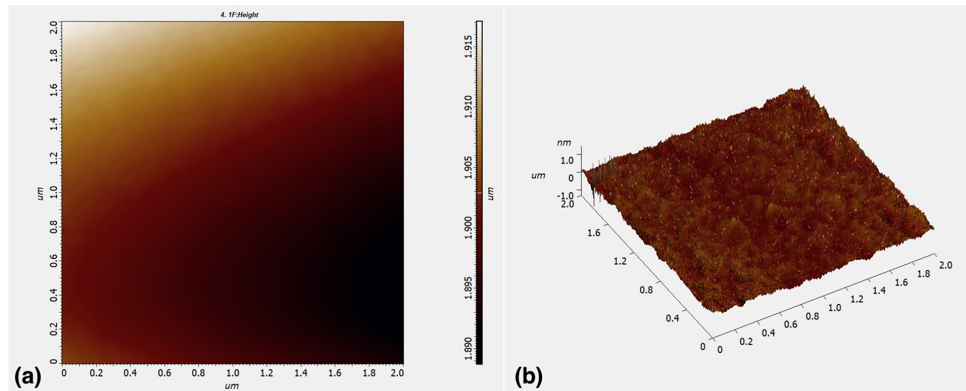

Figure 5.8: AFM diagram of (a) real surface scan of Al_2O_3 and (b) flattened diagram of the surface in 3D form.

regular pattern. These waves are not considered an error of the deposition as they are very small and hence negligible. They were most likely caused by the feedback loop of the AFM system that could have induced frequency on the sample in coincidence with the scanning frequency. Altogether both measured thin films exhibited very good uniform coating, SiO_2 film slightly better than Al_2O_3.

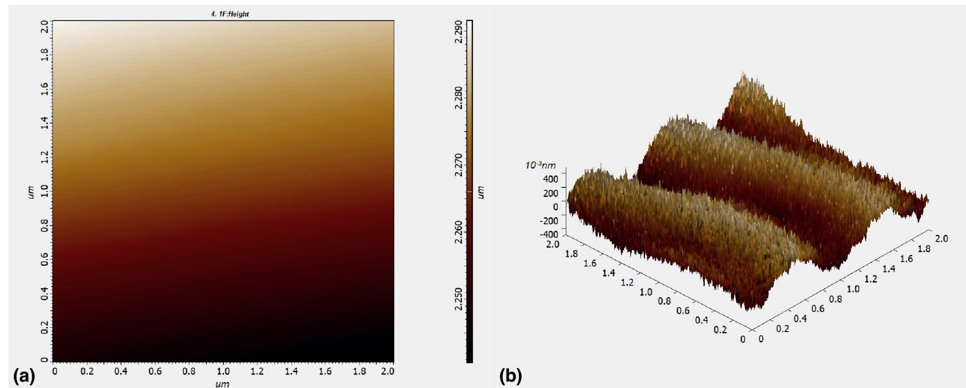

Figure 5.9: AFM diagram of (a) real surface scan of SiO_2 and (b) flattened diagram of the surface in 3D form.

5.5 Capacitor Experiment

As an additional demonstration of the PEALD growth, an attempt to create a parallel-plate capacitor was formed, specifically four capacitors with different thicknesses of the dielectricum. The main purpose of this experiment was to deposit a PEALD layer without SENTECH'S supervision correctly; the

precision of the creation of capacitor electrodes was henced less significant in this experiment. PEALD was used to deposit a dielectric layer of Al_2O_3 onto an aluminum electrode. The final product was again subjected to Raman spectroscopy and AFM, and the capacitance of the complete capacitor was measured on LCR Bridge HM8118 from the HAMEG company.

The process began with four pieces (rectangles of approx. 3.5 cm × 2.5 cm surface) of glass being wholly coated with aluminum Al by a thermal evaporation system. The system used for the evaporation was Q150T Turbomolecular pumped coater by Quorum. Then one half of each piece was covered with thermal-resistant tape. Together, these samples were put into the PEALD reactor and were taken out one by one after four different deposition. A thin film of Al_2O_3 was deposited onto the Al electrodes in the same way as in Chapter 5.2 via the same recipe. Table 5.2 shows how many cycles were run for each sample and a computed final thickness of the layers. After

Number of cycles	Thickness
50	5.5 nm
182	20 nm
455	50 nm
909	100 nm

Table 5.2: Samples' PEALD characteristics

the PEALD process, the samples were let to cool down, and the tape was removed. The tape left a trace at the edge of the newly coated layer that can be seen in Figure 5.10.

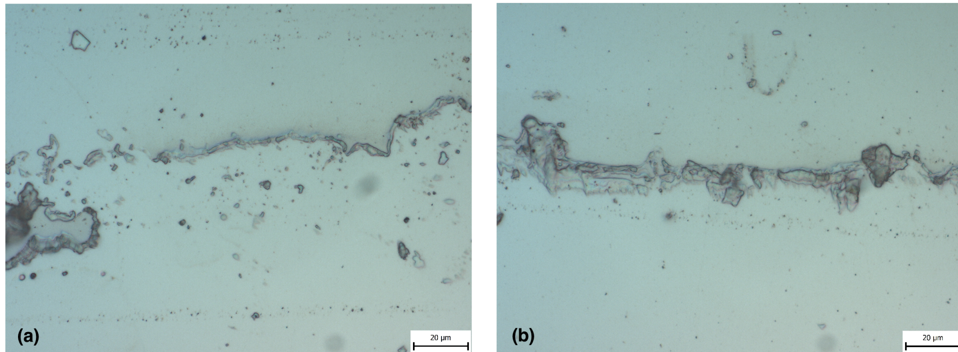

Figure 5.10: The border between Al and Al_2O_3 with tape impurities under regular microskope: (a) for 20 nm sample (b) for 100 nm sample.

All these samples were examined by AFM, the 100 nm layer piece was captured on Figure 5.11 (a), on the Al_2O_3 coated part. The majority of the surface reports about 100 nm in height differences with singular peaks with up to 300 nm difference. The second measurement was taken on the borderline of Al and Al_2O_3 with the hope of seeing the thickness increase on the oxide part. Indeed, in the middle of Figure 5.11 (b), where the border is clearest, a

change of color and thus height can be observed.

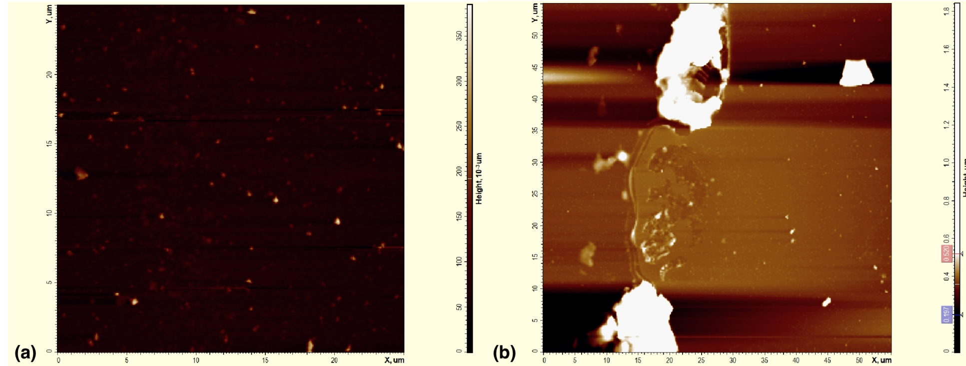

Figure 5.11: AFM diagram of (a) the Al_2O_3 layer and (b) the border between Al and Al_2O_3 with tape impurities.

With the same AFM software, a height profile was created for the 20 nm and the 100 nm sample. The 20 nm profile shows a slight elevation of about 10-20 nm; however, the 100 nm profile shows only 30 nm elevation. Moreover, when conducting this measurement, it was found out that the elevated part of the sample switched to the other side when the imaging direction was changed. Therefore, the measurement is most likely invalid, for the tape remnants highly deflected the tip scanning process.

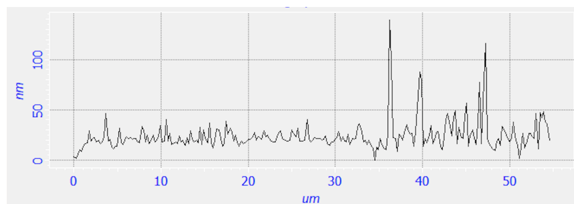

Figure 5.12: Height profile of the surface of the 20 nm capacitor.

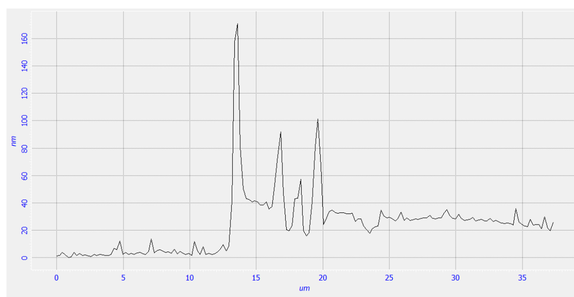

Figure 5.13: Height profile of the surface of the 100 nm sample with Al_2O_3 coating.

The next step in the experiment was a deposition of the upper electrode. The four samples were covered with tape on all sides, so only small squares of the oxide layer were left visible. The samples were again put into the thermal evaporation system, and according to the system software, a 58 nm thick

layer of Al was deposited onto them. The tape was removed from the samples, leaving them in a final form, as seen in Figure 5.14.

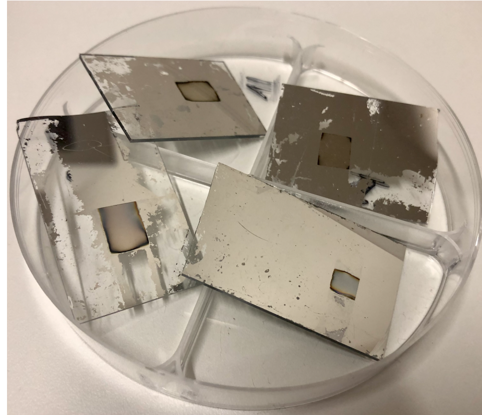

Figure 5.14: The four samples after the second Al layer deposition.

All samples underwent a capacitance measurement. Only one sample with capacitance emerged out of this measurement; the rest came out as conductors. The functional capacitor was the 20 nm layer sample, and the capacitance was 4 pF. This number sadly does not match the capacitor parameters. Considering the standard capacitance formula

$$C = \varepsilon \, \frac{S}{d}, \tag{5.1}$$

the permittivity and the capacitance are both determined and known, leaving the S and d parameters for discussion. If the proper implementation of PEALD leading to 20 nm thickness is considered, the area S equals $7{\cdot}10^{-10}$ m, which is much smaller than the real area of the upper electrode, approximately 24 mm^2. A proposed conclusion is that the second aluminum layer was not uniformly applied, leaving grains of Al on the oxide surface. According to the previous calculation, such grain would be 30 μm wide in diameter, which could fit into the physical reality.

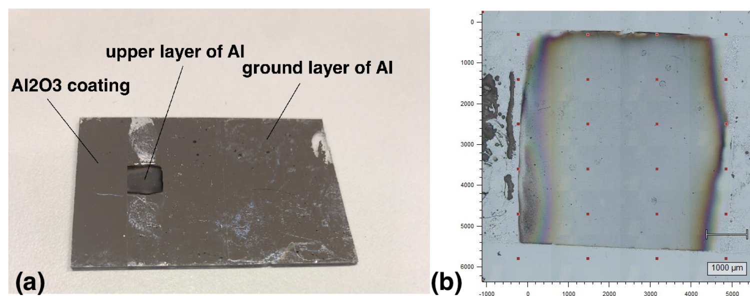

Figure 5.15: (a) Photo of the sample with 20 nm functional capacitor. (b) The 20 nm capacitor under Raman microscope.

Conclusions

Electronic devices are becoming smaller and increasingly structured with complex 3D shapes, needing a controllable deposition of conformal thin films. ALD can meet these demands with sequential self-limiting reactions while being one of the most effective methods on the market. ALD processes have been exploited for a wide variety of materials, and yet new materials and technologies like spatial ALD, allowing faster depositions speeds, are being actively developed. The demand for precise deposition techniques has never been higher, identifying ALD as a crucial developing instrument for emerging nanofabrications.

In this thesis, the basics principles of ALD were described, and many advantages of ALD were highlighted. An overview of a broad range of ALD applications was given, focusing on the transistor and non-volatile memory devices. A commercial ALD system from SENTECH was introduced in more detail and operated in the experimental part, where a successful ALD deposition of thin films was conducted. Grown Al_2O_3 and SiO_2 films were examined, demonstrating the ALD characteristical features. From another partially successful experiment, one functional, though underperforming, parallel-plate capacitor emerged.

While proposing an exciting future of ALD worldwide, the ALD system at the Faculty of Electrical Engineering laboratory has its own bright future as well. The new laboratory also includes a plasma-etching system, presenting a powerful duo with ALD in creating original-shaped structures with broad coating possibilities. In cooperations with research teams in the Department of Microelectronics and other Czech academic institutions, the growth of

thin high-κ dielectrics films, protecting passivation coating of electronic parts, sensory layers based on ZnO, TiO_2, and many more applications will be investigated and developed.

Bibliography

[1] RICHARD W. JOHNSON, ADAM HULTQVIST, STACEY F. BENT, *A brief review of atomic layer deposition: from fundamentals to applications.* Materials Today, vol. 17, Issue 5, 2014, pp. 236–246, ISSN 1369-7021.

[2] ARTO PAKKALA, MATTI PUTKONEN, *27 - Atomic Layer Deposition,.* William Andrew Publishing, 2010, pp. 364-391, ISBN 9780815520313.

[3] H.C.M. KNOOPS, S.E. POTTS, A.A. BOL, W.M.M. KESSELS, *Chapter 8 - Atomic Layer Deposition, Handbook of Crystal Growth (Second Edition).* North-Holland, 2015, pp. 1101-1134, ISBN 9780444633040.

[4] KIM HYUNG JUN, LEE HAN-BO-RAM, W.-J- MAENG, *Applications of atomic layer deposition to nanofabrication and emerging nanodevices.* Thin Solid Films, vol. 517, Issue 8, 2009, pp. 2563–2580, ISSN 0040-6090.

[5] ERWIN KESSELS, *Overview of all materials prepared by atomic layer deposition (ALD).* [Online, accessed from `https://www.atomiclimits.com/wp-content/uploads/2019/02/Periodic-table-ALD-Feb2019.pdf` February, 2019].

[6] S.E. POTTS, W.M.M. KESSELS, *Energy-enhanced atomic layer deposition for more process and precursor versatility*, Coordination Chemistry Reviews, Volume 257, Issues 23–24, 2013, pp. 3254-3270, ISSN 0010-8545.

[7] ADRIE MACKUS, *Approaches, challenges and opportunities for area-selective ALD*, Handouts, Eindhoven University of Technology, Tutorial ALD 2017.

[8] M. M. FRANK, G. D. WILK et al., *HfO_2 and Al_2O_3 gate dielectrics on GaAs grown by atomic layer deposition*, Appl. Phys. Lett. 86, 2015, 152904

[9] P. PUNCHAIPETCH, Y. URAOKA et al., *Enhancing memory efficiency of Si nanocrystal floating gate memories with high-κ gate oxides*, Appl. Phys. Lett. 89, 2006, 093502

[10] BERND GRUSKA, *Low temperature deposition of thin passivation layers by plasma ALD*, Handouts to CTU, SENTECH Instruments GmbH, Germany.

[11] B. GRUSKA, H. Gargouri, M. Arens*Real Time True Surface Monitoring for ALD Processes*, Handouts from Workshop on ALD, 7. 10. 2014, SENTECH Instruments GmbH, Germany.

[12] SENTECH Instruments GmbH *SI ALD LL Atomic Layer Deposition with Load lock, Product description*, Handouts to CTU, SENTECH Instruments GmbH, Germany.

[13] SENTECH Instruments GmbH*Atomic Layer Deposition System SI ALD (LL)*, Operation Manual, Version 1.4, May 2015, SENTECH Instruments GmbH, Germany.

[14] SENTECH Instruments GmbH*ALD Real Time Monitor*, User Manual, October 2015, SENTECH Instruments GmbH, Germany.

[15] PICOSUN^{TM}*Industrial ALD Product Line*, Brochure, 2016, PICOSUN^{TM}, Finnland.

[16] PICOSUN^{TM}, *Picosun's ALD technology enables record capacitance density (...)* [Online, accessed from `https://passive-components.eu/picosuns-ald-technology-enables-3d-silicon-integrated-micr_ocapacitors-with-unprecedented-performance/` 20. 4. 2020].

[17] PICOSUN^{TM}, *PICOSUN R-200 Advanced* [Online, accessed from `https://www.picosun.com/product/r-200-advanced/` 7. 5. 2021].

[18] Veeco, *Fiji - Plasma Enhanced ALD for R&B* [Online, accessed from `https://www.veeco.com/products/fiji-plasma-enhanced-ald-for-rd/` 7. 5. 2021].

[19] SENTECH Instruments GmbH, *Atomic Layer Deposition Systems* [Online, accessed from `https://www.sentech.com/en/ALD-Systems__2492/` 7. 5. 2021].

[20] MITTLER TOLEDO, *Raman Spectroscopy.* [Online, accessed from `https://www.mt.com/au/en/home/applications/L1_AutoChem_Applications/Raman-Spectroscopy.html#overviewaf` 8. 5. 2021].

[21] EDINBURGH INSTRUMENTS, *What is Raman Spectroscopy?.* [Online, accessed from https://www.edinst.com/blog/what-is-raman-spectroscopy/ 8. 5. 2021].

[22] RENISHAW, *inVIa Qontor confocal Raman microscope.* [Online, accessed from https://www.renishaw.com/media/thumbnails/320wide/45f0e05befac4cedae5ab894c1b55078.jpg 8. 5. 2021].

[23] NT-MDT Spectrum Instruments, *NTEGRA.* [Online, accessed from https://www.ntmdt-si.com/data/media/images/products/ntegra/prima/integra_new.jpg 8. 5. 2021].

[24] nanoScience Instruments, *Atomic Force Microscopy.* [Online, accessed from https://www.nanoscience.com/techniques/atomic-force-microscopy/ 8. 5. 2021].

[25] nanoScience Instruments, *Atomic Force Microscopy.* [Online, accessed from https://www.nanoscience.com/wp-content/uploads/2018/04/Laser-beam-deflection-for-Atomic-Force-Microscopes.png 8. 5. 2021].

[26] SUPRAKAS SINHA RAY, *4 - Techniques for characterizing the structure and properties of polymer nanocomposites.* Series in Composites Science and Engineering, Environmentally Friendly Polymer Nanocomposites, Woodhead Publishing, 2013, pp. 74-88, ISBN 9780857097774.

[27] YUNPING LAN, YONGGANG ZOU, XIAOHUI MA, LI XU, LINLIN SHI AND JIABIN ZHANG, *Fabrication of amorphous Al_2O_3 optical film with various refractive index and low surface roughness.* Materials Research express, vol. 7, number 8, 2020, pp. 086405,

[28] C. WIRTZ, T. HALLAM, C. P. CULLEN, N. C. BERNER, M. O'BRIEN, M. MARCIA, A. HIRSH and G. S. DUESBERG *Atomic layer deposition on 2D transition metal chalcogenides: layer dependent reactivity and seeding with organic ad-layers.* Chemical Communications, Issue 92 2015, pp. 16553 —16556.

ZADÁNÍ BAKALÁŘSKÉ PRÁCE

I. OSOBNÍ A STUDIJNÍ ÚDAJE

Příjmení: **Veselá** Jméno: **Karolína** Osobní číslo: **483890**

Fakulta/ústav: **Fakulta elektrotechnická**

Zadávající katedra/ústav: **Katedra radioelektroniky**

Studijní program: **Otevřené elektronické systémy**

II. ÚDAJE K BAKALÁŘSKÉ PRÁCI

Název bakalářské práce:

Depozice atomárních vrstev

Název bakalářské práce anglicky:

Atomic Layer Deposition (ALD)

Pokyny pro vypracování:

1. Seznamte se s obecnými principy růstu vrstev pomocí ALD a jejich konkrétními aplikacemi v elektronice.
2. Seznamte se s parametry a obsluhou konkrétního zařízení od firmy Sentech.
3. Proveďte růst testovací tenké oxidové vrstvy a charakterizujte její povrchové vlastnosti pomocí optického mikroskopu a mikroskopu AFM.

Seznam doporučené literatury:

[1] R. W. Johnson, A. Hultqvist, S. F. Bent: A brief review of atomic layer deposition: from fundamentals to applications, Materials Today, sv. 17, č. 5, str. 236-246, 2014
[2] H. Kim, H. Lee, W.-J. Maeng: Applications of atomic layer deposition to nanofabrication and emerging nanodevices, Thin Solid Films, sv. 517, str. 2563–2580, 2009
[3] H. Li et al.: Enhanced electrical properties of dual-layer channel ZnO thin film transistors prepared by atomic layer deposition, sv. 439, str. 632-637, 2018

Jméno a pracoviště vedoucí(ho) bakalářské práce:

doc. RNDr. Jan Voves, CSc., katedra mikroelektroniky FEL

Jméno a pracoviště druhé(ho) vedoucí(ho) nebo konzultanta(ky) bakalářské práce:

Datum zadání bakalářské práce: **22.01.2021** Termín odevzdání bakalářské práce: ______________

Platnost zadání bakalářské práce: **30.09.2022**

doc. RNDr. Jan Voves, CSc.	doc. Ing. Josef Dobeš, CSc.	prof. Mgr. Petr Páta, Ph.D.
podpis vedoucí(ho) práce	podpis vedoucí(ho) ústavu/katedry	podpis děkana(ky)

III. PŘEVZETÍ ZADÁNÍ

Studentka bere na vědomí, že je povinna vypracovat bakalářskou práci samostatně, bez cizí pomoci, s výjimkou poskytnutých konzultací. Seznam použité literatury, jiných pramenů a jmen konzultantů je třeba uvést v bakalářské práci.

.	
Datum převzetí zadání	Podpis studentky

© VUT v Praze, Design: VUT v Praze, VIC